Investigation of Long-term Voltage Stability Considering a Voltage-Reactive Power Droop Characteristic

Mojtaba Momeni [1], Maik Schönefeld [1], Albert Moser [1]

[1] Institute for Electrical Equipment & Grids, Digitalization & Energy Economics (IAEW), RWTH Aachen University, Aachen, Germany, m.momeni@iaew.rwth-aachen.de

Abstract: This paper proposes an expansion of the Newton-Raphson method applied in the steady-state power flow calculations to include a more accurate modeling of the reactive power capabilities of renewable energy sources (RESs) connected at the EHV/HV interfaces. The voltage control capability of synchronous generation units is typically modeled via PV buses in the steady-state power flow problem resulting in QV curves with an infinite slope. However, the reactive power exchange of the converter-coupled RESs with the grid is usually a function of the measured operating voltage at the point of common coupling (PCC). The reactive power injection thus results from the measured voltage at the PCC and the parameters of droop the characteristic curve. In practice, the reference voltage is changed to enable a different reactive power exchange at the connection point. The results show that the maximum loading can be increased when a droop bus formulation is used to model the reactive power contribution of the converter-coupled RESs. Furthermore, it can be seen that a droop bus approximates the behavior of a PV bus when a small droop coefficient is given. Besides, the continuation power flow (CPF) is used to calculate the system transition path between discrete operating points. It can be shown that the maximum and minimum voltages remain constrained between the discrete upper and lower voltage bounds once a droop characteristic is considered to adjust the reactive power contribution of the RESs within the transition.

Keywords: Reactive Power Droop Control, Voltage Control, Continuation Power Flow, Transition Path

1 Introduction

Steady-state voltage control in the extra-high voltage grid is normally achieved by provision of reactive power through conventional power plants connected to block transformers or reactive power compensation devices such as mechanically switched capacitors (MSCs) or reactors (MSRs) in order to maintain the voltage magnitudes within the prescribed limits. In addition, renewable energy sources such as wind and large-scale photovoltaic plants connected at the EHV/HV interfaces should have the capability to provide controllable reactive power as requested by grid codes [6]. While synchronous machines are capable of providing reactive power almost instantaneously, power plants based on RES coupled with converters exchange reactive power with the grid following a voltage-reactive power droop characteristic. In other words, their reactive power injection is a function of the current operating voltage at the point of common coupling [2]. The conventional approach to model a droop characteristic via a slack, PV or PQ bus in a power flow is invalid since neither the reactive power nor the voltage magnitude of a droop bus are known quantities beforehand. Therefore, an accurate modeling of the voltage-reactive power droop characteristic necessitates the expansion of the

conventional power flow problem to incorporate the droop linear dependency into the equations. To that end, the power mismatch equations as well as the Jacobian matrix are modified to include additional terms resulting from the droop characteristic. This paper also proposes an expansion of the continuation power flow method taking into account the voltage-reactive power droop characteristic and is structured as follows: The formulation and modeling of the droop bus are presented in chapter 2. Chapter 3 provides the simulation results of the proposed method on a benchmark case. Conclusions are given in chapter 4.

2 Modeling

2.1 Droop Bus

The bus type in a power flow problem depends on the pre-specified quantities. Table I provides an overview on the classification of bus types and is expanded by an additional row pertaining to the droop bus. In comparison to the classical definition, where at each bus two quantities are known and two are to be determined, only the active power injection of a droop bus is pre-specified whereas its voltage magnitude and phase angle together with its reactive power injection are to be calculated. However, the reactive power injection of a droop bus is a linear function of its voltage magnitude and can be written as [3]:

$$Q_G = Q_0 + {}^{1}/_{n_q}\,(V_0 - V) \qquad (1)$$

Table 1: Classification buy types in a power flow

Bus Type	P	Q	V	δ
PQ	known	known	unknown	unknown
PV	known	unknown	known	unknown
Slack	unknown	unknown	known	known
Droop	known	$\propto V$	unknown	unknown

where Q_0 and V_0 are the reactive power and voltage set points, respectively; Q_G and V are the reactive power generation and voltage magnitude of the droop bus, respectively; and n_q is the specified droop coefficient. Therefore, Q_G is a voltage dependent variable and must be updated in each iteration of the Newton-Raphson method.

2.2 Proposed Power Flow Method

In the conventional Newton-Raphson (N-R) method, the calculated values of active and reactive power at each bus are subtracted from the corresponding injected values to form the following mismatch equations:

$$\Delta P_i = P_i^{inj.} - \underbrace{V_i \sum_{j=1}^{n} V_j Y_{ij} \cos(\delta_i - \delta_j - \varphi_{ij})}_{calc.} \qquad (2)$$

$$\Delta Q_i = Q_i^{inj.} - \underbrace{V_i \sum_{j=1}^{n} V_j Y_{ij} \sin(\delta_i - \delta_j - \varphi_{ij})}_{calc.} \qquad (3)$$

where ΔP_i and ΔQ_i are the active and reactive power mismatch equations at bus i, respectively; $\underline{Y_{ij}} = Y_{ij} \measuredangle \varphi_{ij}$ is the sum of all the admittances connected to bus i when $i = j$ and the negative of the sum of all the admittances between bus i and bus j when $i \neq j$; and δ_i and δ_j denote the phase angles at bus i and bus j, respectively.

In the conventional method, the active and reactive power injections do not change in the N-R iterations; however, since the injected reactive power of a droop bus is a function of its voltage magnitude, droop equation (1) is inserted in (3) to get

$$\begin{aligned} &\Delta Q_i^{(k)} \\ &= \overbrace{Q_{0,i} + {}^1\!/_{n_q}\left(V_{0,i} - V_i^{(k)}\right)}^{inj.} \\ &\underbrace{- V_i^{(k)} \sum_{j=1}^{n} V_j^{(k)} Y_{ij} \sin\left(\delta_i^{(k)} - \delta_j^{(k)} - \varphi_{ij}\right)}_{calc.} \end{aligned} \tag{4}$$

where (k) is the iteration index and is introduced here to show that the injected reactive power is updated within each iteration using the bus voltage solution at iteration (k) when i is a droop bus. The injected active power of the droop bus, however, remains unchanged.

Next, the mismatch equations are driven to zero until the calculated power leaving each bus equals the injected power. The N-R method is formulated as

$$\underbrace{\begin{bmatrix} J_1 & J_2 \\ J_3 & J_4 \end{bmatrix}}_{J} \begin{bmatrix} \Delta\delta \\ \Delta V \end{bmatrix} = \begin{bmatrix} \Delta P \\ \Delta Q \end{bmatrix} \tag{5}$$

where $\Delta\delta = \delta^{(k+1)} - \delta^{(k)}$ and $\Delta V = V^{(k+1)} - V^{(k)}$. The Jacobian matrix J is comprised of four smaller submatrices given by

$$\begin{bmatrix} J_1 & J_2 \\ J_3 & J_4 \end{bmatrix} = \begin{bmatrix} \frac{\partial \Delta P}{\partial \delta} & \frac{\partial \Delta P}{\partial V} \\ \frac{\partial \Delta Q}{\partial \delta} & \frac{\partial \Delta Q}{\partial V} \end{bmatrix} \tag{6}$$

The submatrices J_1 and J_2 contain the derivatives of the active power mismatch equations with respect to phase angles and voltage magnitudes, respectively and are not affected as a result of the droop equation. Submatrix J_3 includes the derivatives of the reactive power mismatch equations with respect to phase angles and is not affected, either. J_4 is the only submatrix that contains the derivatives of the reactive power mismatch equations with respect to voltage magnitudes in the form of

$$J_4 = \begin{bmatrix} \frac{\partial \Delta Q_2^{(k)}}{\delta V_2^{(k)}} & \cdots & \frac{\partial \Delta Q_2^{(k)}}{\delta V_i^{(k)}} & \cdots & \frac{\partial \Delta Q_2^{(k)}}{\delta V_n^{(k)}} \\ \vdots & \ddots & \vdots & \ddots & \vdots \\ \frac{\partial \Delta Q_i^{(k)}}{\delta V_2^{(k)}} & \cdots & \frac{\partial \Delta Q_i^{(k)}}{\delta V_i^{(k)}} & \cdots & \frac{\partial \Delta Q_i^{(k)}}{\delta V_n^{(k)}} \\ \vdots & \ddots & \vdots & \ddots & \vdots \\ \frac{\partial \Delta Q_n^{(k)}}{\delta V_2^{(k)}} & \cdots & \frac{\partial \Delta Q_n^{(k)}}{\delta V_i^{(k)}} & \cdots & \frac{\partial \Delta Q_n^{(k)}}{\delta V_n^{(k)}} \end{bmatrix} \tag{7}$$

Taking the derivative of (4) with respect to $V_i^{(k)}$ gives

$$\frac{\partial \Delta Q_i^{(k)}}{\partial V_i^{(k)}} = \frac{-1}{n_q} - \sum_{j=1}^{n} V_j^{(k)} Y_{ij} \sin\left(\delta_i^{(k)} - \delta_j^{(k)} - \varphi_{ij}\right) + V_i^{(k)} Y_{ij} \sin \varphi_{ii} \quad (8)$$

Thus, when i is a droop bus, the diagonal elements of J_4 contain an additional term, which expresses the derivative of the droop equation with respect to the bus voltage magnitude; consequently, the off-diagonal elements of J_4 remain unchanged.

2.3 Reactive Current Droop Control

The reactive current droop expresses the injected reactive current of the droop bus as a function of its voltage magnitude and can be written as

$$I_B = k(V_o - V) \quad (9)$$

where k is the reactive current droop coefficient (not to be mistaken with the iteration index (k)), and I_B is the injected reactive current. Using (9), the injected reactive power Q_G can be obtained as

$$Q_G = I_B \cdot V = k(V_o - V) \cdot V \quad (10)$$

Taking the derivative of (10) with respect to the voltage magnitude, we get

$$\frac{\partial Q_G}{\partial V} = k \cdot V_o - 2k \cdot V \quad (11)$$

Therefore, when the reactive current droop is used, the reactive power mismatch equations and the Jacobian can be modified in a similar fashion to the reactive power droop control to incorporate the behaviors derived in (10) and (11) in obtaining the solution.

2.4 Example of a Droop Characteristic

Let us consider the 3-bus system shown in Figure 1. The system parameters are given in [5]. Bus 2 is defined as a droop bus and the droop coefficient at this bus is set to 0.04. There is one slack generator at bus 1, and bus 3 is a PQ (load) bus. Table II contains the obtained voltage solutions and power injections at each bus using the proposed power flow method.

Table 2: Obtained solutions using the proposed method

Bus	V_{ref}	P_{gen}	Q_{gen}	P_{load}	P_{load}	V	δ
1	1.0	0.7087	0.1484	0.0	0.0	1.0	0.0
2	1.0	0.5	0.0955	0.0	0.0	0.9962	-0.7092
3	—	0.0	0.0	1.2	0.5	0.9691	-3.7898

Using the converged voltage magnitude at bus 2 and substituting it in (1), we can write

$$Q_{G,2} = Q_{0,2} + {}^{1}/_{n_q}\left(V_{0,2} - V_2\right) = 0 + \frac{1}{0.04}(1 - 0.962) = 0.0950 \quad (12)$$

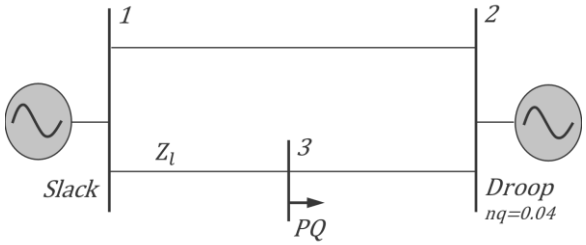

Figure 1: Three-bus system with a droop bus

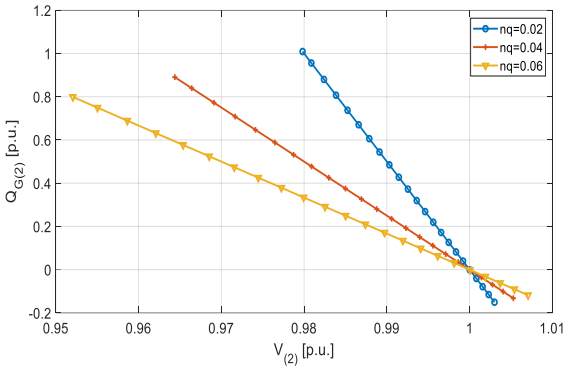

Figure 2: Droop characteristic curves with droop coefficient n_q as a parameter

The droop characteristic curve plots the injected reactive power of the droop bus against the bus voltage magnitude variation. These curves are shown in Figure 2 treating the droop coefficient n_q as a separate parameter. It can be seen that when $n_q = 0.02$, full reactive power (1 p.u.) is released once the bus voltage drops to 0.98 p.u., which is equivalent to a 2% deviation from the set point value. Therefore, only half the reactive power (0.5 p.u.) is released at a 2% voltage deviation when $n_q = 0.04$. In practice, a droop coefficient of 2% to 10% is typically employed [2].

2.5 Network Transition Path

The continuation power flow (CPF) as a curve-tracing tool can also be used to calculate a network transition path between discrete hourly generation and load schedules. The base scenario is created using generation and load powers at the initial hour (current hour) whereas the target scenario uses generation and load powers at the following hour (next hour). Nevertheless, the following issues need to be addressed:

a) Startup and shut down of power plants between two hours shall be modeled.

b) The adaption of transformers off-nominal tap ratios shall be realized.

Startup and shutdown of power plants can be modeled by converting the PV buses connecting these generators into PQ buses while the active and reactive power generations at these buses are ramped up or down to reach the specified target value at the next hour.

Transformers tap ratios can be adjusted by calculating the total number of steps required to reach the target value of the next hour and creating corresponding events, which are triggered

independently from each other to increase or decrease the tap ratios in steps towards the target value.

3 Results

3.1 Benchmark Network

The benchmark network, shown in Figure 3, is based on the IEEE 118-bus network; however, to make it compliant with the European standards, the electrical properties of it have been modified. The topology of the network in terms of the electrical distance between consumers, conventional power plants and the focal points of installed photovoltaic or wind generation features an additional analogy to the German transmission grid.

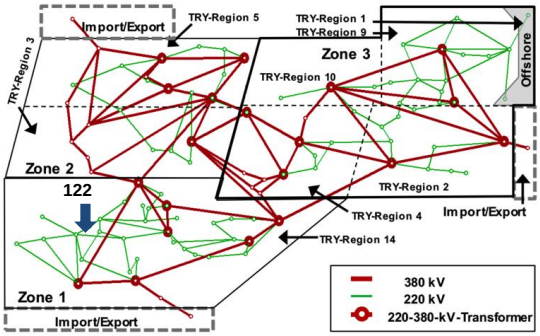

Figure 3: Benchmark network topological representation

It comprises 120 buses in the 220 kV and 380 kV level voltages. The 27 kV level buses, which connect the conventional power plants and 110 kV level buses in the case of aggregated inverter-coupled generation units are not however shown here. The consumers connected to distribution networks are considered in terms of accumulated loads at the 110 kV level buses. Additionally, the model has a temporal component describing the network for an entire year with 8760 discrete points in time or time series for power generation and consumption [1].

3.2 Initialization

In order to assess the impact of reactive power injection from renewable sources on long-term voltage stability, the benchmark network is initialized at 12:00 o'clock on the 15th of August. At this hour, the infeed of power from renewables reaches about 93% of the total generated power.

3.3 The Network Characteristic Curves

The Network PV curves are plotted in Figure 4. The abscissa shows the total active power demand variation and voltage variation is drawn on the vertical axis. Three scenarios are considered as follows:

Scenario I: The 110 kV level buses, which are connected to renewables, are converted from PQ to PV buses.

Scenario II: The 110 kV level buses connecting renewables are converted from PQ to droop buses assuming three values of n_q. It must be noted that $n_q = 0.5$ is an unrealistic value which is only considered for an easier comparison of the curves.

Scenario III: The 110 kV level buses connecting renewables are modeled as PQ buses.

In a power system, the loading margin is defined as the distance between initial and final load values. It corresponds to the maximum load increase which can still be supported by the system without loss of stability [4]. From Figure 4, the following observations can be made:

I. The highest loading margin is achieved when the 110 kV level buses are modeled as PV buses (scenario I).
II. The network loading margin is expanded when droop buses are considered. However, the loading margin decreases as n_q increases towards 0.5.
III. The lowest loading margin is achieved when the 110 kV level buses are modeled as PQ buses (scenario III). Moreover, the voltage magnitude declines more rapidly in this case.

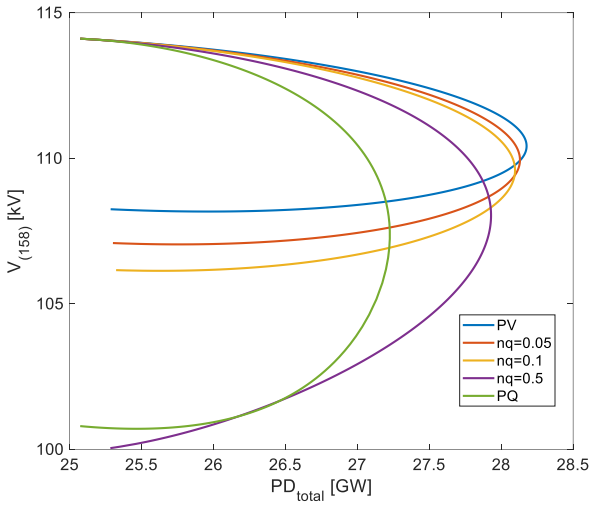

Figure 4: The benchmark network PV curves assuming three values of the droop coefficient

3.4 The Network Transition Path

In Figure 5, the network generation and load powers in a time period from 11:00 to 16:00 are shown in terms of discrete points marked with the orange dots. The aim is to use the CPF to obtain a continuous profile of the network generation and load powers as time progresses. However, as a first step the startup and shut down of conventional powers plants needs to be modeled. Let's consider the generator at bus 122, as shown in Figure 3. The status of this generator in the considered period is given in Table III. As can be seen, there is a startup of this generator in the interval from 11:00 to 12:00. Therefore, this bus is modeled as a PQ bus during this interval in order to increase the active and reactive power injections at this bus linearly towards the specified target values at 12:00 0'clock. Figure 6 illustrates the variation of reactive power generation and the voltage magnitude of this bus during the considered period.

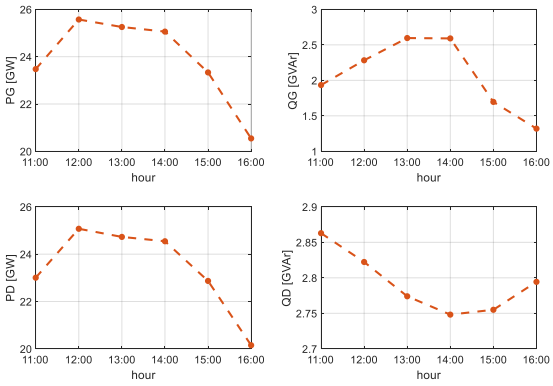

Figure 5: The benchmark network discrete generation and load powers

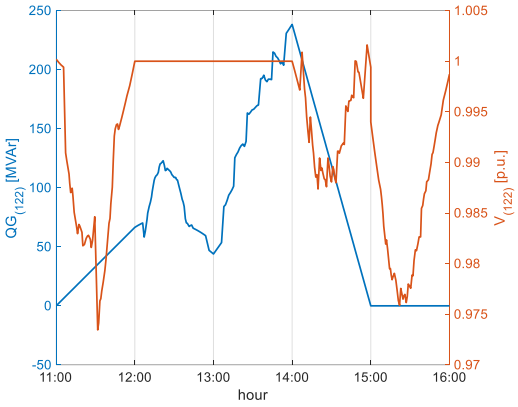

Figure 6: Reactive power generation and voltage magnitude at bus 122 in the benchmark network

Table 3: Generator status at bus 122

Hour	11:00	12:00	13:00	14:00	15:00	16:00
Status	off	on	on	on	off	off

From 12:00 to 14:00, this generator supplies the network with an active and reactive power and the terminal voltage is held constant at 1 p.u. The reactive power is then ramped down towards zero in the interval from 14:00 to 15:00. This generator is shutdown at 15:00 o'clock.

The continuous course of the network generation and load powers are shown in Figure 7. These graphs are obtained using the CPF. However, for comparison the droop buses were not considered first. As can be seen, the active power generation and the load powers are adapted linearly in each interval crossing the discrete points at each hour. The reactive power generation, however, is calculated iteratively within each run of the CPF, but crossing the discrete values at the end of each interval as well. When the droop buses are considered in the calculations, the graphs of Figure 8 are obtained. In comparison to Figure 7, the curve of reactive power generation does not cross the discrete values in this case. This deviation is due to the following: According to (1), in order to avoid any deviation from the discrete power flow results, it is also necessary to adjust the voltage set points of the droop buses within the transition towards the target values of the next hour. However, here, the initial voltage set points at hour 11:00 were applied throughout the transition, which resulted in a small deviation from the discrete power flow results.

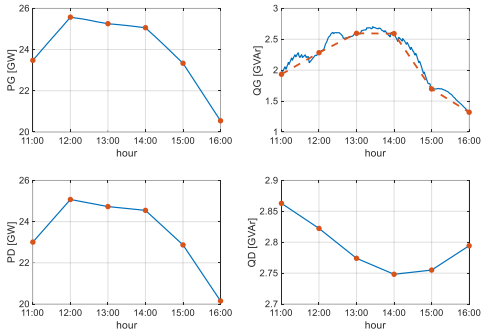

Figure 7: Continous variation of generation and load power without considering the droop characteristic

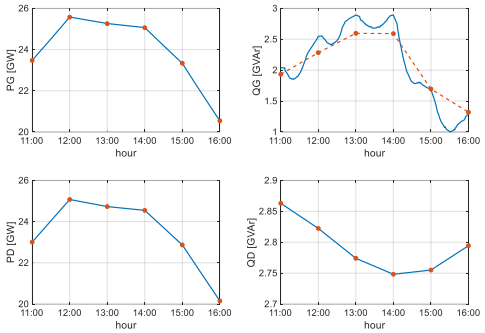

Figure 8: Continous variation of generation and load power considering the droop characteristic

The evolution of voltages in the considered period can also be examined first disregarding the droop characteristic in the calculations. Figure 9 shows the maximum, mean and minimum voltages in the network across the 220 kV and 380 kV level buses. The upper voltage bound is the maximum of the discrete maximum voltages taken at each hour. Similarly, the lower bound is the minimum of the discrete minimum voltages. Without considering the droop buses, the minimum and maximum voltages violate the discrete upper and lower voltage bounds. Taking the droop buses into account, however, the voltages shown in Figure 10 are obtained. In comparison, the maximum and minimum voltages remain constrained between the discrete upper and lower voltage bounds in this case.

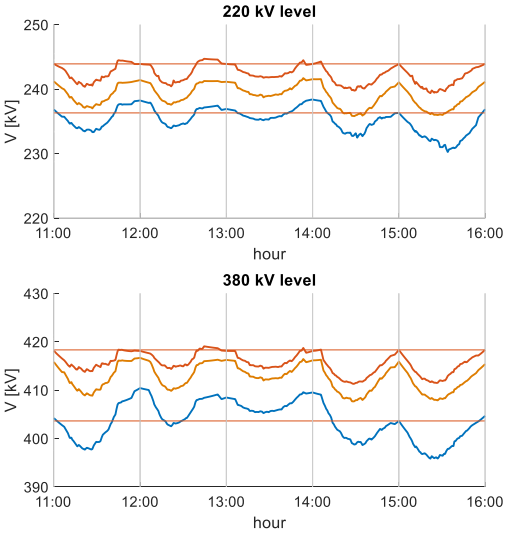

Figure 9: The Evolution of voltages without considering the droop characteristic

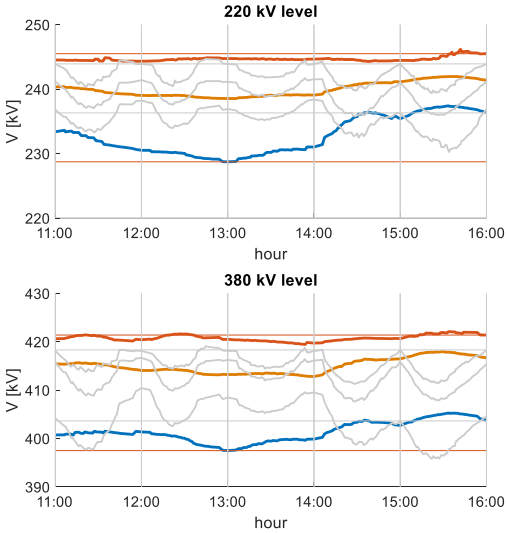

Figure 10: The Evolution of voltages considering the droop characteristic

4 Conclusion

In this paper, the reactive droop characteristic of inverter-coupled generating units is integrated in the power flow calculations by introducing a new bus type called droop bus. The droop bus follows its voltage set point by adjusting its reactive power output. The droop coefficient determines the sensitivity of a droop bus with respect to voltage deviations. For small droop coefficients close to 2%, the droop bus approximates the behavior of a PV bus. The model

was tested on a benchmark case and the network PV curves were obtained. The results confirm that the network loading margin is extended when the droop buses are considered. Furthermore, the network transition path between discrete generation and load powers is calculated using the CPF. To that purpose, the startup and shut down of conventional power plants between consecutive hours are modeled via ramping up or down generation and load powers at the corresponding generators towards the target values. Transformers off-nominal tap ratio variations are also represented using a step-wise adaption of the ratios towards the defined target values at the next hour. The results show that without considering the droop buses, the minimum and maximum voltages exceed the discrete upper and lower voltage bounds, repeatedly; however, when the droop buses are considered, the voltages remain constrained between the discrete bounds during the transition period.

References

[1] Barrios, H., Roehder, A., Natemeyer, H., and Schnettler, A. 2015 - 2015. A benchmark case for network expansion methods. In *2015 IEEE Eindhoven PowerTech*. IEEE, 1–6. DOI=10.1109/PTC.2015.7232601.

[2] Ellis, A., Nelson, R., Engeln, E. von, MacDowell, J., Casey, L., Seymour, E., and Peter, W. 2012 - 2012. Reactive power performance requirements for wind and solar plants. In *2012 IEEE Power and Energy Society General Meeting*. IEEE, 1–8. DOI=10.1109/PESGM.2012.6345568.

[3] Mumtaz, F., Syed, M. H., Hosani, M. A., and Zeineldin, H. H. 2016. A Novel Approach to Solve Power Flow for Islanded Microgrids Using Modified Newton Raphson With Droop Control of DG. *IEEE Transactions on Sustainable Energy* 7, 2, 493–503.

[4] van Cutsem, T. and Vournas, C. 2008. *Voltage stability of electric power systems*. Power Electronics and Power Systems Series. Springer, New York.

[5] Venkata, S. S. 2011. Computational Methods for Electric Power Systems (Crow, M. L., Ed; 2010) [Book Reviews]. *IEEE Power and Energy Mag.* 9, 2, 78–80.

[6] VDE-AR-N 4130 (VDE-AR-N 4130) Anwendungsregel: 2018-11